ACS APPLIED MATERIALS & INTERFACES

Forum Article

www.acsami.org

# Mechanically Strong, Flexible Polyimide Aerogels Cross-Linked with Aromatic Triamine

Mary Ann B. Meador,*[,†] Ericka J. Malow,[†] Rebecca Silva,[†] Sarah Wright,[†] Derek Quade,[‡] Stephanie L. Vivod,[†] Haiquan Guo,[‡] Jiao Guo,[§] and Miko Cakmak[§]

[†]NASA Glenn Research Center, 21000 Brookpark Road, Cleveland, Ohio 44135, United States

[‡]Ohio Aerospace Institute, 22800 Cedar Point Road, Cleveland, Ohio 44142, United States

[§]University of Akron, Akron, Ohio 44325, United States

**ABSTRACT:** Polyimide gels are produced by cross-linking anhydride capped polyamic acid oligomers with aromatic triamine in solution and chemically imidizing. The gels are then supercritically dried to form nanoporous polyimide aerogels with densities as low as 0.14 g/cm$^3$ and surface areas as high as 512 m$^2$/g. To understand the effect of the polyimide backbone on properties, aerogels from several combinations of diamine and dianhydride, and formulated oligomer chain length are examined. Formulations made from 2,2′-dimethylbenzidine as the diamine shrink the least but have among the highest compressive modulus. Formulations made using 4,4′-oxydianiline or 2,2′dimethylbenzidine can be fabricated into continuous thin films using a roll to roll casting process. The films are flexible enough to be rolled or folded back on themselves and recover completely without cracking or flaking, and have tensile strengths of 4−9 MPa. Finally, the highest onset of decomposition (above 600 °C) of the polyimide aerogels was obtained using *p*-phenylene diamine as the backbone diamine with either dianhydride studied. All of the aerogels are suitable candidates for high-temperature insulation with glass transition temperatures ranging from 270−340 °C and onsets of decomposition from 460−610 °C.

**KEYWORDS:** *aerogel, polyimide, cross-linking, nanoporous materials, high-temperature insulation*

## INTRODUCTION

Aerogels are highly porous solids characterized by very small pore sizes and large internal surface areas, making them excellent as thermal insulators, catalyst supports, filtration devices, etc.[1] However, the most widely studied silica aerogels tend to be quite fragile because of the nature of their skeletal structure. Mechanical properties of silica aerogels are improved by applying a conformal coating of polymer to the silica backbone.[2] Unfortunately, polymers such as epoxy,[3] isocyanate,[4] cyanoacrylates,[5] and styrene,[6] typically used for reinforcement tend to be stable up to at most 100−150 °C. For many aerospace applications, such as insulation for launch vehicles or for planetary entry, descent, and landing (EDL) systems,[7] much higher use temperatures are needed.

For EDL applications in particular, a high degree of flexibility or even foldability of the insulation as part of a layered construct is required so that a large inflatable can be packaged in a small space to later deploy into a lightweight heat shield/decelerator.[8] EDL systems were used to land robotic missions on Mars, employing hard aeroshell heat shields and parachutes of 12−16 m in diameter. Future robotic and manned missions will be much heavier and will require more drag for landing, dictating inflatable aerodynamic decelerators with much larger diameters (30−60 m) to perform the same function.[9]

Because of their thermal stability, good mechanical properties, and high glass transition temperatures, polyimides are the polymer of choice for applications such as aircraft engines needing high performance at elevated temperatures.[10−12] Drawing on this large body of work, it would be ideal to design polyimide aerogels with a good combination of properties for use as high-temperature, lightweight, flexible insulation required for EDL systems.

Previously, polyimide aerogels have been synthesized by gelation of chemically imidized polyimides in dilute solution, followed by supercritical drying.[13,14] In this approach, the aerogels had a strong tendency to shrink during processing up to as much as 40%. The latter paper included an alternate approach to polyimide aerogel synthesis using reaction of dianhydrides with di-isocyanates instead of diamines. This approach resulted in less shrinkage if the polymer gels were allowed to cure at room temperature, but weight loss at 200 °C from thermal gravimetric analysis revealed that this results in much less than complete imidization. Polyimide aerogels have also been synthesized by cross-linking anhydride capped

**Received:** October 23, 2011
**Accepted:** December 22, 2011
**Published:** January 10, 2012

  

**Scheme 1. General Synthesis Route for Polyimide Aerogels Cross-Linked with TAB**

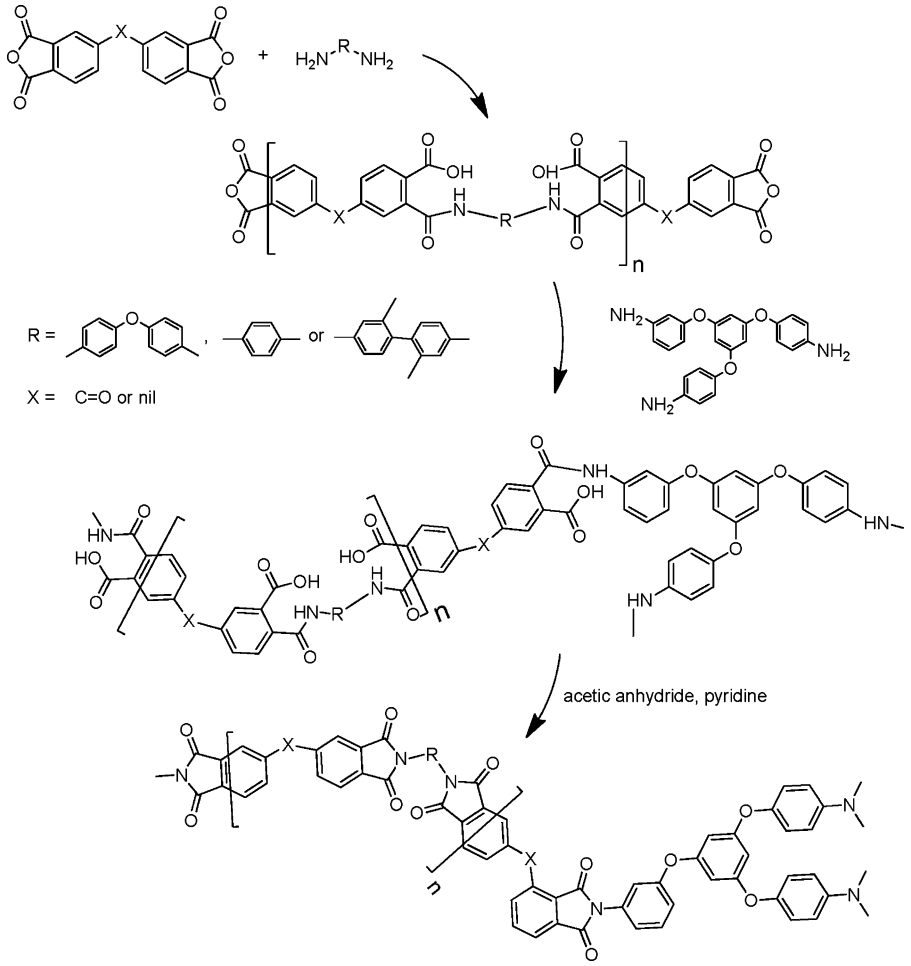


polyamic acid oligomers through aromatic triamines and thermally imidizing.[15,16] These aerogels exhibited very little shrinkage and up to 90% porosity. However, the gels tended to re-dissolve during thermal imidization and reform upon cooling, obviating the need to keep the gels in molds. This is not conducive to fabrication of free standing films using roll-to-roll processing, and also suggests that some of the amic acid hydrolyzes during thermal imidization, which breaks up the network structure.

Recently, we have reported the preparation of polyimide aerogels cross-linked through octa(aminophenyl) silsesquioxane (OAPS) units.[17] These organic aerogels can be produced with very little shrinkage during the processing and have thermal conductivity comparable to silica aerogels of similar density (only 14 mW/(m K) for aerogels with density of 0.1 g/cm$^3$) but are much stronger with compressive modulus ranging from 1 to 5 MPa. Most notably, these aerogels can be fabricated as thin films that are flexible and foldable, and are stable up to 400 °C for short term exposure. In fact, initial testing of these aerogels in a layered insulation system demonstrated survivability with a laser heat flux load of 20 W/cm$^2$ for 90 s.[18] In this test, the layup included two layers of ceramic woven fabric on top of eleven layers of the thin film OAPS cross-linked polyimide aerogel (total thickness of 3 mm). The heat flux resulted in an upper surface temperature of 1200 °C, whereas the temperature under the bottom-most aerogel layer was less than 300 °C. Although these results are promising, only one type of polyimide backbone derived from bisaniline-*p*-xylidene (BAX) and biphenyl-3,3′,4,4′-tetracarboxylic dianydride (BPDA) was examined. Properties such as high temperature stability and mechanical strength may be improved further by examining other diamines and dianhydrides typically used in polyimides for aircraft engine components and other high-temperature applications.

Herein, we re-examine the approach of cross-linking through an aromatic triamine, 1,3,5-triaminophenoxybenzene (TAB) in place of OAPS, producing a three-dimensional, covalently bonded network structure according to Scheme 1. However, similar to the process used for OAPS cross-linked polyimide aerogels, we use chemical imidization at room temperature with pyridine/acetic anhydride to yield fully imidized cross-linked gels that are supercritically dried from liquid $CO_2$ to produce the aerogels. TAB was first used in polyimide synthesis by Stille to create star-shaped oligomers with better melt processing.[19] More recently, TAB has been used to make highly branched polyimides for battery electrolytes[20] and for separation membranes.[21] In the latter cases, steps were taken to avoid gelation, whereas for creating the aerogels, a balanced stoichiometry and no end-capping are used to promote gelation. A series of TAB cross-linked aerogels derived from three different diamines—*p*-phenylene diamine (PPDA), 2,2′-dimethylbenzidine (DMBZ), and 4,4′-oxydianiline (ODA)—and two different dianhydrides—benzophenone-3,3′,4′4′-tetracarboxylic dianhydride (BTDA) and (BPDA)—were examined.


dx.doi.org/10.1021/am2014635 | ACS Appl. Mater. Interfaces 2012, 4, 536−544

Table 1. Formulations and Properties of Polyimide Aerogels Cross-Linked with TAB

| sample | no. of repeats, *n* | diamine | dianhydride | density ($g/cm^3$) | porosity (%) | shrinkage (%) | BET surface area ($m^2/g$) | modulus (MPa) | onset of decomposition (°C) | $T_g$ (°C) |
|---|---|---|---|---|---|---|---|---|---|---|
| 1 | 15 | ODA | BPDA | 0.206 | 88.0 | 24.5 | 377 | 15.9 | 558 | 274 |
| 2 | 20 | ODA | BPDA | 0.194 | 86.7 | 22.4 | 401 | 11.1 | 557 | 267 |
| 3 | 25 | ODA | BPDA | 0.194 | 88.1 | 22.8 | 412 | 12.7 | 548 | 272 |
| 4 | 15 | ODA | BTDA | 0.144 | 90.6 | 20.3 | 469 | 1.0 | 552 | 257 |
| 5 | 20 | ODA | BTDA | 0.167 | 89.5 | 20.3 | 499 | 1.5 | 567 | 271 |
| 6 | 25 | ODA | BTDA | 0.157 | 89.4 | 19.3 | 477 | 0.9 | 565 | 268 |
| 7 | 15 | ODA | BPDA | 0.181 | 90.1 | 21.2 | 425 | 16.9 | 555 | 255 |
| 8 | 20 | ODA | BPDA | 0.196 | 86.2 | 22.1 | 377 | 5.5 | 552 | 272 |
| 9 | 25 | ODA | BPDA | 0.180 | 87.5 | 21.1 | 362 | 12.2 | 550 | 267 |
| 10 | 15 | ODA | BTDA | 0.192 | 87.0 | 23.3 | - | 0.9 | 560 | 278 |
| 11 | 20 | ODA | BTDA | 0.207 | 86.0 | 25.0 | 503 | 2.3 | 550 | 282 |
| 12 | 15 | PPDA | BPDA | 0.318 | 79.8 | 47.8 | 335 | 30.1 | 600 | 346 |
| 13 | 20 | PPDA | BPDA | 0.333 | 77.6 | 47.9 | 329 | 46.1 | 609 | 343 |
| 14 | 25 | PPDA | BPDA | 0.324 | 79.5 | 47.1 | 255 | 19.1 | 593 | - |
| 15 | 15 | PPDA | BTDA | 0.231 | 84.9 | 41.4 | 358 | 27.6 | 566 | 337 |
| 16 | 20 | PPDA | BTDA | 0.210 | 86.2 | 39.7 | 498 | 19.2 | 571 | 321 |
| 17 | 25 | PPDA | BTDA | 0.219 | 85.0 | 40.2 | 461 | 29.2 | 570 | 325 |
| 18 | 30 | DMBZ | BPDA | 0.146 | 89.7 | 19.0 | 314 | 19.1 | 517 | 286 |
| 19 | 30 | DMBZ | BTDA | 0.195 | 87.1 | 27.5 | 442 | 58.4 | 463 | - |
| 20 | 30 | DMBZ | BPDA | 0.131 | 91.6 | 17.1 | 472 | 20.1 | 511 | 293 |
| 21 | 30 | DMBZ | BTDA | 0.181 | 87.6 | 30.1 | 340 | 102 | 470 | - |
| 22 | 30 | ODA | BPDA | 0.207 | 86.3 | 28.7 | 202 | 13.9 | 577 | 292 |

These diamines and dianhydrides were chosen because they are all readily available and are known to impart different properties to the polyimides.[12] For example, using BPDA, PPDA, and DMBZ produces a rigid backbone in the polyimide structure, leading to higher glass transition temperatures, whereas ODA and BTDA have flexible linking groups between phenyl rings resulting in less rigid structures. Thus, another goal of this work is to examine the effects of these backbone structures on the properties of polyimide aerogels.

## EXPERIMENTAL SECTION

**Materials.** 1,3,5-Triaminophenoxybenzene (TAB) was obtained from Triton Systems (200 Turnpike Rd # 2, Chelmsford, MA 01824-4053). Pyridine, acetic anhydride, *p*-phenylene diamine (PPDA), and anhydrous N-methylpyrrolidinone (NMP) were purchased from Sigma Aldrich. 2,2′-Dimethylbenzidine (DMBZ), 4,4′-oxydianiline (ODA), benzophenone-3,3′,4′4′-tetracarboxylic dianhydride (BTDA), and biphenyl-3,3′,4,4′-tetracarboxylic dianydride (BPDA) were obtained from Chriskev, Inc. (13920 W 108th Street, Lenexa, Kansas, 66215). Dianhydrides were dried at 125 °C in vacuum for 24 h before use. All other reagents were used without further purification.

**Instrumentation.** Attenuated total reflectance (ATR) infrared spectroscopy was conducted using a Nicolet Nexus 470 FT-IR spectrometer. $^{13}C$ NMR spectra of the polymers were obtained on a Bruker Avance 300 spectrometer using 4 mm solids probe with magic angle spinning at 11 kHz and cross-polarization. Spectra were externally referenced to the carbonyl peak of glycine (176.1 ppm relative to TMS). A Hitachi S-4700 field emission microscope was used for the scanning electron microscope (SEM) images after sputter coating the specimens with gold. The samples were outgassed at 80° C for 8 h under vacuum before running nitrogen−adsorption porosimetry with an ASAP 2000 surface Area/Pore Distribution analyzer (Micromeritics Instrument Corp.) The skeletal density was measured using a Micromeritics Accupyc 1340 helium pycnometer. Thermal gravimetric analyses (TGA) was performed using a TA model 2950 HiRes instrument. Samples were run at a temperature ramp rate of 10 °C per min from room temperature to 750 °C under nitrogen and air. Glass transition temperatures were obtained using a TMA 2940 thermomechanical analyzer from TA Instruments.

**Synthesis of Polyimide Aerogels Using Chemical Imidization.** Polyimide aerogels were prepared as shown in Scheme 1. Aerogels from three different diamines (ODA, DMBZ, or PPDA) and two different dianhydrides (BPDA or BTDA) with the formulated number of repeat units, n, varied between 15 and 30, were prepared according to Table 1 as 10 wt % solutions of polyimide in NMP. As an example, preparation of $n$ = 30 polyimide aerogel using BPDA, TAB and ODA (Table 1, run 22) is described. To a solution of ODA (3.16 g, 15.8 mmol) in 50 mL of NMP under nitrogen was added BPDA (4.79 g, 16.3 mmol). After all the BPDA dissolved, a solution of TAB (0.14 g, 0.35 mmol) in 16 mL of NMP was added with stirring. After 10 min of stirring, acetic anhydride (12.3 mL, 130 mmol, 8:1 molar ratio to BPDA) and pyridine (10.5 mL, 130 mmol) were added to the solution. Immediately after mixing, the solution was poured into prepared molds. The solution gelled within 20 min. The gels were aged for 24 h in the mold. Following aging, the gels were extracted into a solution of 75 % NMP in acetone and soaked overnight. Subsequently, the solvent was exchanged in 24 h intervals with 25 % NMP in acetone, and finally 100 % acetone. The solvent was removed by supercritical $CO_2$ extraction, followed by vacuum drying overnight at 80 °C, resulting in polyimide aerogels having a density of 0.203 g/$cm^3$. $^{13}C$ CPMAS NMR (ppm): 124.4, 130.7, 143.2, 155, 165.6. FT-IR: 1774.7, 1718.2, 1501.0, 1374.8, 1241.4, 1170.3, 1115.3 1087.8, 878.9, 830.0, 737.6.

Thin film fabrication was carried out using a roll-to-roll casting system. The same 10 w/w % NMP solution as above was cast onto a PET carrier film running at a speed of 80 cm/min using a 12 in. wide Doctor blade with front opening gap set at 1.09 mm. The film that gelled within 30 min was sealed in a plastic bag and aged for 24 h before peeling away from the PET carrier. Afterwards, the films were washed in 24 h intervals in 75 % NMP in acetone, followed by 25 % NMP in acetone and finally in 100 % acetone. Supercritical drying gave polyimide aerogel thin films (0.45 mm) with similar properties to above.

**Compression Tests.** The specimens were tested in accordance with ASTM D695-10 with the sample sizes nominally 1.5−1.8 cm in diameter and 3 cm in length (close to the 1:2 ratio of diameter to length prescribed for the testing of polymer foams). The samples were tested between a pair of compression platens on a model 4505 Instron load frame using the Series IX data acquisition software. The platen

surfaces were coated with a graphite lubricant to reduce the surface friction and barreling of the specimen.

**Tensile Tests.** Thin film specimens nominally 5 mm wide by 33 mm long were mounted on a rectangular paperboard frame using adhesive tape as shown in the inset for Figure 8. This setup supports and aligns the flexible film to install on the Instron 5567 load frame controlled with Bluehill software. The sides of the paperboard were cut after mounting and before the test. Tensile tests were run using 100 N load and an extension speed of 2 mm/min based on ASTM D882. Reported tensile properties are the average of six tests.

**Statistical Analyses.** Experimental design and analyses were conducted using Design Expert Version 8.1, available from Stat-Ease, Inc., Minneapolis, MN. Multiple linear regression analysis was used to derive empirical models to describe the effect of each of the process variables studied on measured properties. Full quadratic models including all main effects, second-order effects and all two way interactions was entertained, and continuous variables were orthogonalized (transformed to −1 to +1 scale) before analysis. Terms deemed to not be significant in the model (<90 % confidence) were eliminated one at a time using a backward stepwise regression technique.

## RESULTS AND DISCUSSION

Polyimide aerogels with TAB cross-links were synthesized as shown in Scheme 1. Polyamic acid oligomers capped with anhydride were formed in solution. Enough TAB was added with stirring to react with anhydride end-caps, followed by addition of an eight fold excess of acetic anhydride and pyridine to effect chemical imidization and gelation at room temperature. It should be noted that it is the addition of TAB not imidization catalyst that induces gelation, because a polyamic acid cross-linked network forms as shown in Scheme 1 even without the addition of acetic anhydride and pyridine as previously reported.[16] For this reason, the catalysts must be added soon after addition of TAB before the solution phase separates in order to obtain a homogeneous solution and accordingly a homogeneous gel.

Because NMP is not as soluble in supercritical $CO_2$ and is therefore difficult to remove directly, the solvent in the gels was exchanged to acetone in a series of steps before supercritical drying. Solid NMR spectra of the polyimide aerogels showed them to be free of solvent after drying. Selected NMR spectra of three sample formulations are shown in Figure 1. All spectra contain an imide carbonyl peak at 165 ppm as well as broad aromatic peaks between 115 and 140 ppm characteristic of these polyimides. Aerogels made from ODA as diamine (top spectrum) also have a peak at 155 ppm characteristic of the aromatic ether carbon. Aerogels made using DMBZ as diamine (middle and bottom spectra) give an aliphatic peak at 19 ppm for the pendant methyl groups. Finally, aerogels made using BTDA have an additional peak at 193 ppm characteristic of the benzophenone carbonyl.

Figure 2 shows a picture of typical aerogels made using TAB as a cross-linker. The aerogels are light yellow to orange yellow in appearance. Thin films (nominally 0.5 mm) of the aerogels from certain formulations are flexible—the films can be rolled or folded backward on themselves and completely recover with no evidence of cracking or flaking. Thicker parts such as the 6.5 cm × 6.5 cm × 1.3 cm rectangular prism shown in Figure 2a are rigid and strong, even able to support the weight of a car as seen in Figure 2b (although more rigorous compression testing is described *vide infra*).

Properties of polyimide aerogels made from three different diamines and two dianhydrides with n formulated from 15 to 30 are listed in Table 1. This range was studied because gels made from shorter oligomers (lower formulated n) reacted too

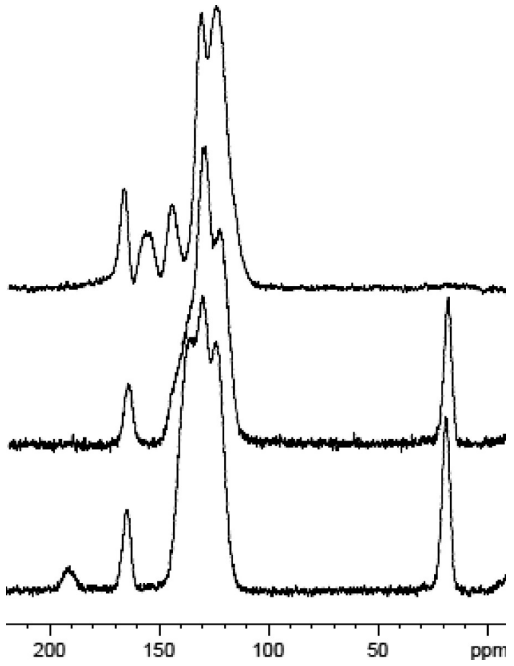


**Figure 1.** Solid NMR of selected formulations of polyimide aerogels showing (top) sample 22 made with BPDA/ODA, (middle) sample 20 made with BPDA/DMBZ, and (bottom) sample 21 made with BTDA/DMBZ.

**Figure 2.** (a) Polyimide aerogels cross-linked with TAB shown fabricated as flexible thin films or molded to a net shape, and (b) demonstrating strength by supporting the weight of a car.

quickly for incorporation of catalyst for chemical imidization before phase separation occurs. Formulations made using ODA and DMBZ were made from 10 w/w % solutions, whereas because of very fast gelation times, the PPDA samples had to be made from less concentrated 5 w/w % solutions. Analyzing the data using multiple linear least squares regression gives empirical models of the effect of the significant variables on the measured properties of the aerogels. For almost all measured responses, the formulated number of repeat units, n, in the range of 15 to 30, was not found to be a significant factor in the models over and above random error. Thus, the data are presented as bar graphs showing the effect of diamine and dianhydride on the modeled responses with error bars representing the standard deviation of the regression.

Shrinkage occurs during fabrication of the aerogels, mostly during initial gelation but some additional shrinkage may occur on solvent exchange and supercritical drying. It might be expected that using PPDA or DMBZ in the polymer backbone would help the gels resist shrinkage, since both make the polymer backbone more rigid. This is not the case. As seen in


dx.doi.org/10.1021/am2014635 | ACS Appl. Mater. Interfaces 2012, 4, 536−544

Figure 3a, shrinkage (standard deviation = 1.92 %, $R^2$ = 0.97) is more pronounced in aerogels made using PPDA (40+ %)

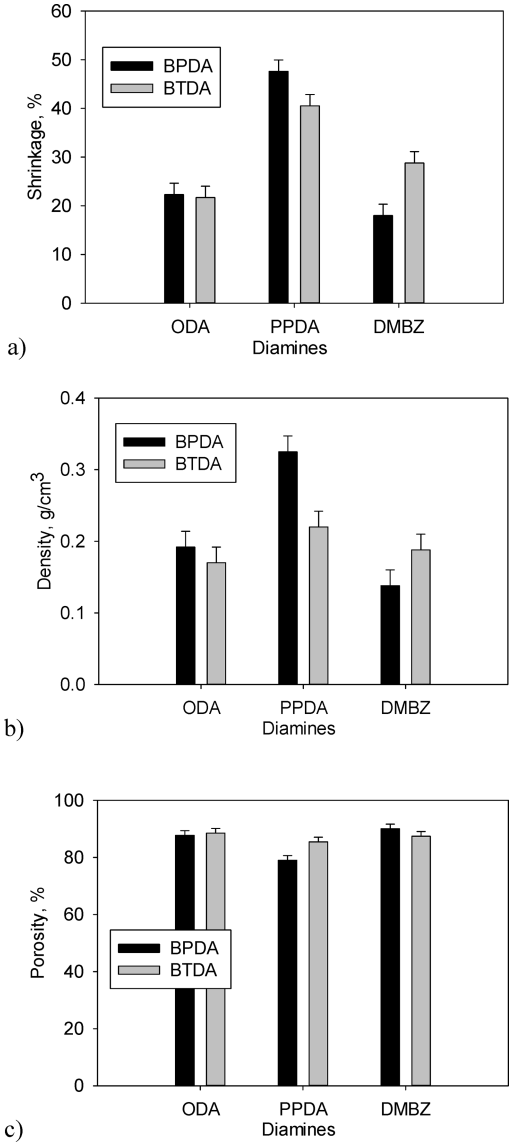


**Figure 3.** Properties of polyimide aerogels cross-linked with TAB including: (a) average shrinkage during processing; (b) average density; and (c) average porosity. Error bars represent one standard deviation calculated by statistical modeling of all data.

compared to those made from ODA or DMBZ (17-30%). The least amount of shrinkage was seen for aerogels made using the combination of DMBZ and BPDA. Since most of the shrinkage occurs during gelation (polymer formation), greater shrinkage in PPDA derived polyimide aerogels may in part be due to the ability of the polymer chains to pack more closely together compared to polyimides made with either DMBZ or ODA. Figure 4 compares three dimensional renderings of $n$ = 2 oligomers of BPDA with PPDA, DMBZ, or ODA derived from geometry optimization calculations using MM2.[22] The oligomers are shown with colors representing atoms residing in different planes. Note that the atoms of oligomers from PPDA and BPDA are the same color (red) through almost two repeat units, indicating a high degree of planarity. In contrast, the methyl groups in DMBZ force the phenyl rings to be out of plane with a torsional angle of 75° as measured by X-ray crystallography[23] and therefore DMBZ-BPDA oligomers are non-coplanar. It is well-known that non-coplanarity in the polyimide backbone induces different relaxation behavior,[24] leads to higher solubility[25] and some microporosity[26] in polyimide films and composites. It is plausible that this also induces less shrinkage during gelation attributable to less interaction between polymer chains or to the greater solubility. Oligomers produced using ODA are also non-coplanar due to the oxygen linking groups between the phenyl rings and also exhibit lower shrinkage with either dianhydride, even though this is not a rigid structure. Lower shrinkage here may be due to interaction of the polar solvent with the oxygen link of ODA during gelation. If the oxygen links keep the growing polymer chains from phase separating for longer time, perhaps the network structure that finally forms is better able to resist shrinkage. On the other hand, shrinkage is on the average 7−8 % lower when BTDA is combined with PPDA compare to that of BPDA-PPDA, but is 10 % higher for BTDA-DMBZ compared to BPDA-BMBZ. Clearly, shrinkage is more complex than described herein, with solvent interactions, rigidity of the chains, and interaction between chains possibly all playing a part.

As expected, aerogel densities as shown in Figure 3b (standard deviation = 0.016 g/cm$^3$, $R^2$ = 0.94) echo the shrinkage. Highest densities are produced from PPDA as diamine, especially when BPDA is the dianhydride (0.33 g/cm$^3$). Lowest densities result from the combination of BPDA and DMBZ (0.14 g/cm$^3$). Porosity of the aerogels shown in Figure 3c (standard deviation = 1.41 %, $R^2$ = 0.88) is also influenced by shrinkage with the lowest porosities resulting from aerogels containing PPDA (78-86%). All of the other polyimide aerogel formulations ranged from 86 to 90% porous.

Interestingly, the pore structure as observed by SEM shown in Figure 5 for the aerogels produced using different diamines and dianhydrides are quite dissimilar. Aerogels derived from BPDA (image a, ODA; image c, PPDA; and image e, DMBZ) all appear as collections of polymer strands ranging from 30-50 nm in thickness. The amount of porosity evidenced in each of these micrographs is commensurate with the amount of shrinkage as previously discussed with the combination of PPDA-BPDA showing the least porosity, and the DMBZ-BPDA showing the most porosity. The combination of BTDA and ODA (Figure 5b) produced aerogels that are the most reminiscent of silica aerogels with clusters of 50−100 nm particles loosely connected together. The combination of BTDA with DMBZ (Figure 5f) also appears as clusters of nanoparticles, but the particle sizes are smaller (~50 nm) and more uniform.

Differences in pore structure are also reflected in the surface area measurements made by nitrogen sorption using the Brunauer−Emmet−Teller (BET) method.[27] Figure 6a shows a plot of the average surface areas for different combinations of diamine and dianhydride. The model for surface area (standard deviation = 55 m$^2$/g, $R^2$ = 0.7) is the only one in the study where formulated number of repeat units, n, has a significant effect. In this case, increasing formulated n significantly reduces surface area by about 75 m$^2$/g over the whole range. For comparison sake, in the plot in Figure 6a, average surface areas are shown for $n$ = 30 formulated oligomers. Note that surface areas on the average are significantly larger (~80 m$^2$/g) for BTDA aerogels than those made from BPDA. Aerogels made using DMBZ with either BTDA or BPDA have the largest


dx.doi.org/10.1021/am2014635 | ACS Appl. Mater. Interfaces 2012, 4, 536−544

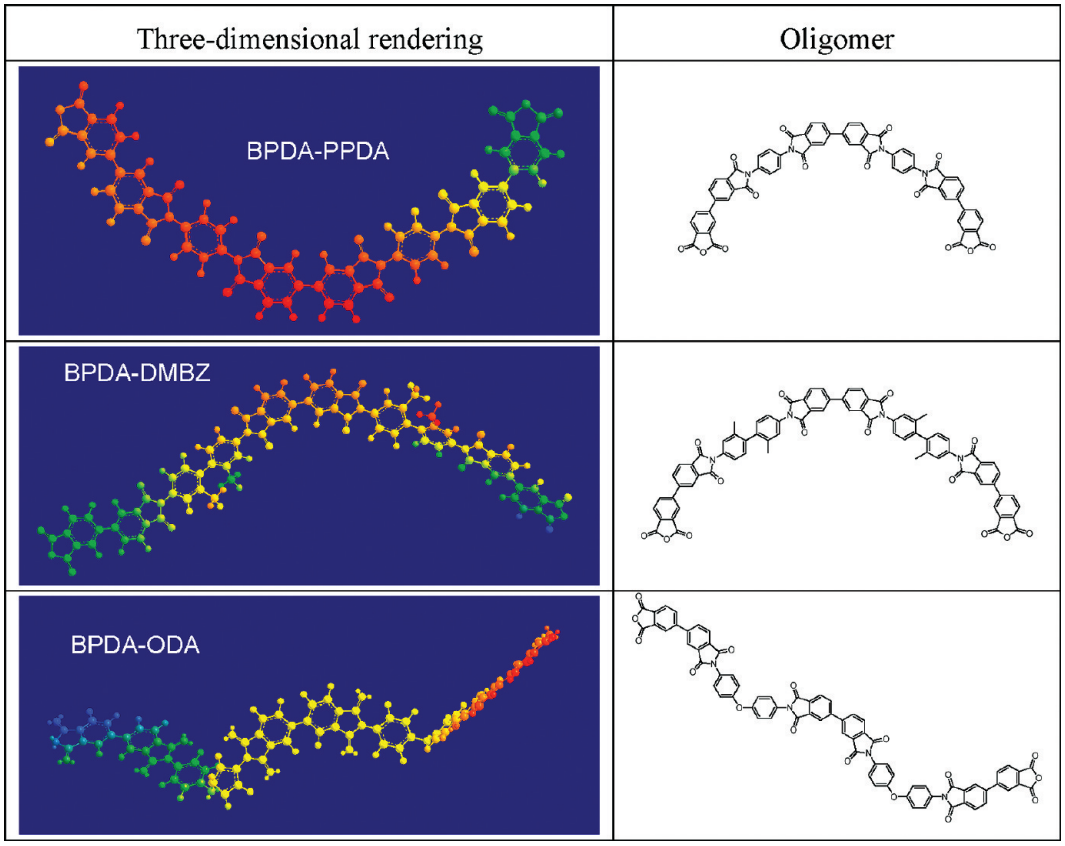


**Figure 4.** Three-dimensional renderings of polyimide oligomers from BPDA and various diamines derived from geometry optimization using MM2. In the renderings, atoms of the same color occupy the same plane.

surface areas while use of PPDA significantly reduces surface area. It might be expected that the same solvent interactions, chain rigidity and coplanarity also have a role in surface area, since this characteristic should also arise from the way the polymer chains pack together. Average pore diameters for BTDA aerogels (Figure 6b, dotted lines) made with PPDA and DMBZ tend to be small (on the order of 10-20 nm) with a sharp pore size distribution. In comparison, aerogels made from a combination of BTDA and ODA have a broader, bimodal pore size distribution, ranging from below 10 nm to almost 100 nm. Pore size distribution for aerogels made with BPDA (Figure 6b, solid lines) and PPDA is similar to that of BTDA, whereas peaks for DMBZ and ODA aerogels with BPDA are shifted to larger pore diameters. Pore sizes seen in the SEMs, especially for aerogels made from the combination of DMBZ-BPDA shown in Figure 5e, appear larger than values measured by nitrogen sorption−desorption. Note that this technique is not sensitive to pores larger than 100 nm. The smaller pores measured by this technique may also be contained within the polymer strands or particles, and would not be visible in the SEMs.

Stress−strain curves from compression testing of select formulations of polyimide aerogels are shown in Figure 7a. Stress−strain curves are similar to those of silica and polymer reinforced silica aerogels with a linear elastic region up to about 4−5 % strain and exhibiting yield up to about 40−50 % strain.[28] Young's modulus taken as the initial slope of the stress strain curve of the aerogels made from different diamines and dianhydrides is shown in Figure 7b (log standard deviation =0.38, $R^2$ = 0.95). For aerogels, in general, modulus increases with increasing density. For the polyimides, highest average modulus is seen for aerogels made from DMBZ and BTDA which are not the highest density aerogels produced in the study. In fact, aerogels made from DMBZ and BPDA are among the lowest density and have average modulus rivaling the highest density PPDA aerogels. This is surprising in that PPDA and DMBZ aerogels both have a stiff backbone structure, so it might be expected that modulus would be similar at similar density. Higher average modulus in DMBZ containing aerogels could be due to more complete polymerization as has been seen in comparison of modulus in other studies of polyimides.[23] Mechanical properties in silica aerogels are also known to depend on better connectivity between particles (more complete reaction).[29] In fact, mathematical modeling and re-evaluation of percolation theory has shown that some of the mass of the aerogel may be dangling mass and not contributing to the overall strength of the material.[30] This has also been demonstrated experimentally for epoxy-reinforced silica aerogels where optimal flexural strength was reached at less than the highest density aerogels reported. It was shown by NMR that incomplete reaction leading to dangling epoxy chains contributed to the greater density but not to increased strength.[31] None of the analyses (DSC, FT-IR, or TGA) indicate differences in extent of imidization, though slight differences could have a significant effect on mechanical properties.

Continuous polyimide aerogel thin films can be fabricated using a roll to roll casting method from 10 w/w % solutions in NMP as previously described.[17] Formulations made from ODA or DMBZ and BPDA and a formulated $n$ = 30, form flexible films as shown in Figure 2. Typical stress-strain curves from tensile testing of these ODA-BPDA and DMBZ-BPDA films


dx.doi.org/10.1021/am2014635 | ACS Appl. Mater. Interfaces 2012, 4, 536−544

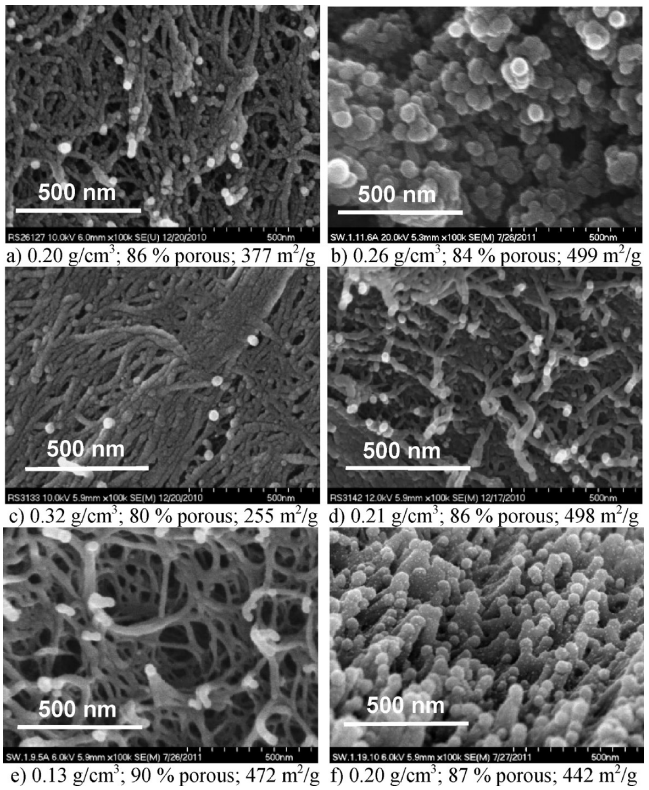


**Figure 5.** SEM of chemically imidized polyimide aerogels from (a) ODA/BPDA, $n$ = 20; (b) ODA/BTDA, $n$ = 20; (c) PPDA/BPDA, $n$ = 25; (d) PPDA/BTDA, $n$ = 20; (e) DMBZ/BPDA, $n$ = 30; and (f) DMBZ/BTDA, $n$ = 30.

are shown in Figure 8a. Note that ODA films break at lower stress but at higher tensile strain than DMBZ films. Figure 8b shows a comparison of tensile modulus and tensile stress at yield for each of the films. Tensile modulus taken as the average of five tests is 23 MPa (standard deviation = 5.4) for ODA films, while that of DMBZ films is 217 MPa. Average tensile stress at break is 4.1 MPa (standard deviation = 0.4) for ODA films and 8.7 MPa (standard deviation = 0.93). As previously mentioned (*vide supra*) the films can be rolled or folded back on themselves and fully recover without any ill effects. Films using ODA can take a crease whereas DMBZ films crack easier on creasing.

Comparisons of the thermal behavior of the aerogel formulations are shown in Figure 9. As seen in Figure 9a, the formulations with the highest onset of decomposition (standard error =7.8 °C, $R^2$ = 0.96) are made using PPDA and BPDA. Formulations made using ODA have a slightly lower onset of decomposition because of the oxygen linkages, whereas DMBZ has the lowest onset because of the pendant methyl groups. BTDA containing formulations degrade at a slightly lower temperature than BPDA formulations. These observations are in agreement with previous studies of thermal stability of polyimides in bulk (non-porous) form.[12,32,33] Average glass transition temperature, $T_g$ shown in Figure 9b (standard error = 10 °C, $R^2$ = 0.89), depends only on diamine used in the formulation (dianhydride is not seen to have a significant effect on average $T_g$ in this study above and beyond standard error). Formulations made from PPDA have the highest average $T_g$ (334 °C) with DMBZ formulations about 40 °C lower at 290 °C. Formulations containing ODA with the more flexible oxygen linking group have the lowest average $T_g$ (271 °C). These trends are also consistent with $T_g$ measured for bulk polyimides.[12,34]

## CONCLUSIONS

A method to fabricate polyimide aerogels with a covalently bonded network structure, using a combination of aromatic diamines and aromatic dianhydrides cross-linked with TAB is described. These aerogels are potentially useful as high-temperature insulation material for various aerospace applications, including EDL applications, launch vehicles, etc. The formulations with the highest thermal stability and glass transition temperatures were made using PPDA as the diamine. However, these formulations tended to shrink the most during gelation, perhaps because of better packing between polymer chains or lower solubility during polymerization (faster phase separation), leading to higher densities and lower porosity. The least shrinkage was observed in aerogels made using DMBZ as the diamine and BPDA as dianhydride. Although these formulations have the lowest densities and highest surface areas of all the formulations studied, compressive modulus is nearly as high as the PPDA formulations which have double the density. In comparison to previously reported polyimide aerogels cross-linked using OAPS, the lowest density DMBZ formulation cross-linked with TAB has a density about 26 % higher, but modulus increases by a factor of 4 and surface areas are also significantly higher for these TAB cross-linked aerogels. This makes these aerogels candidates for multifunctional sandwich structures where a combination of light weight, insulation, high temperature stability and good mechanical

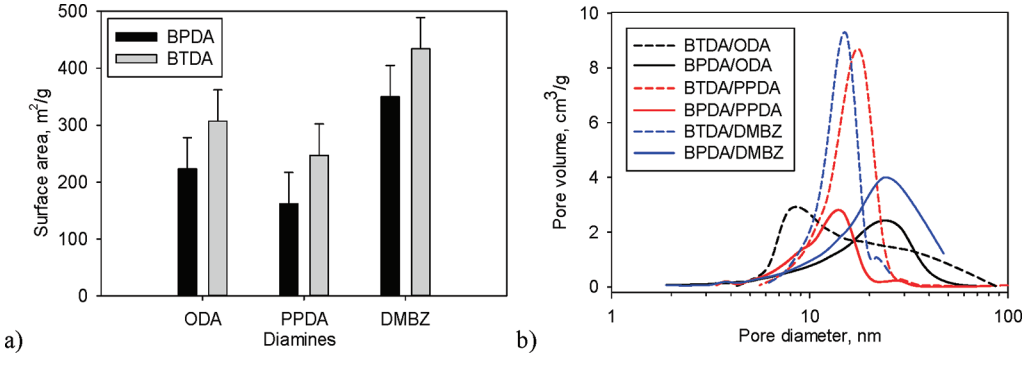


**Figure 6.** Graphs of (a) average surface areas for $n$ = 30 polyimide aerogels with error bars representing one standard deviation from fitted models, and (b) pore size distributions for different formulations.


dx.doi.org/10.1021/am2014635 | ACS Appl. Mater. Interfaces 2012, 4, 536−544

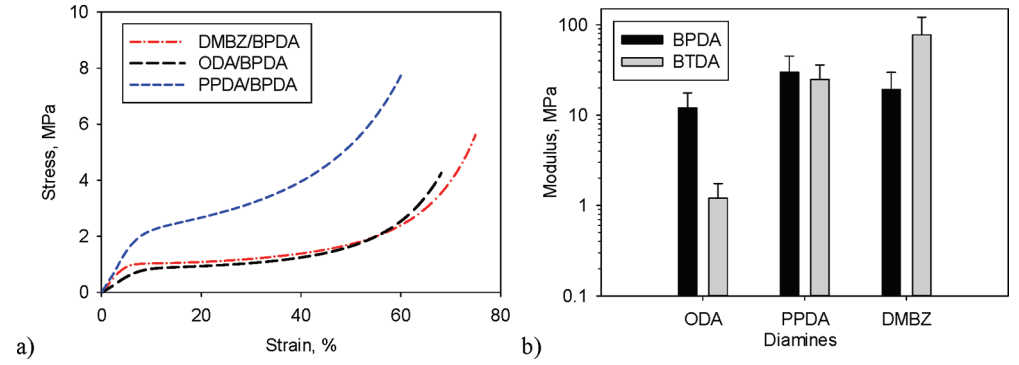


**Figure 7.** Graphs of (a) stress–strain curves from compression for selected polyimide aerogels, and (b) comparison of average Young's Modulus for different formulations with error bars representing one standard deviation from fitted models.

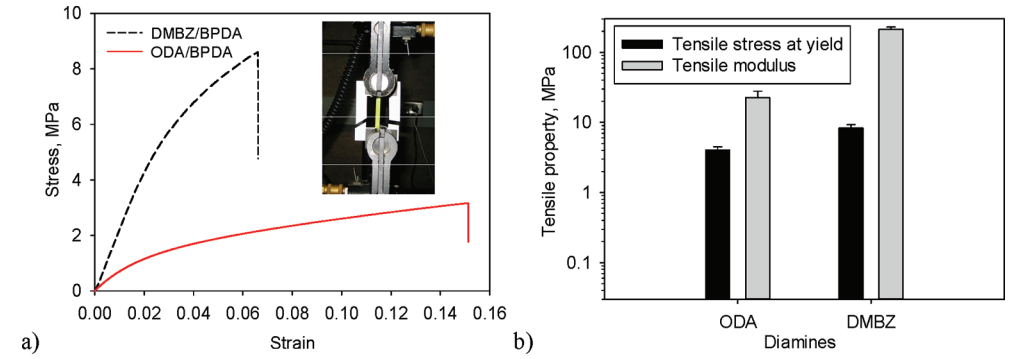


**Figure 8.** (a) Stress–strain curve from typical tensile testing of ODA-BPDA and DMBZ-BPDA polyimide aerogel cross-linked using TAB with inset showing a specimen mounted in the load frame. (b) Comparison of average tensile modulus and average tensile stress at yield between polyimide aerogels made with different diamines.

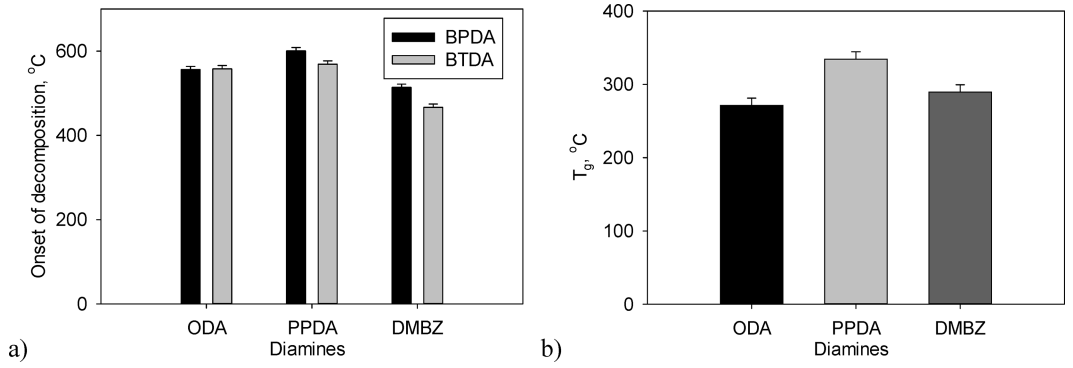


**Figure 9.** Graphs of (a) average onset of decomposition as measured by TGA in nitrogen and (b) average glass transition temperature from TMA of polyimide aerogels cross-linked with TAB. Error bars represent one standard deviation from fitted models.

integrity are needed. Finally, TAB cross-linked formulations made using ODA or DMBZ as diamine and BPDA as dianhydride can be fabricated into thin, flexible films with good tensile properties, making them potential candidates for insulation for inflatable aerodynamic decelerators for EDL applications, inflatable habitats, or extravehicular activity suits as well as more earth-based applications.

## AUTHOR INFORMATION

### Corresponding Author

*E-mail: maryann.meador@nasa.gov.

## ACKNOWLEDGMENTS

We thank the NASA Fundamental Aeronautics Program (Hypersonics) for financial support of this research. In addition, we thank Dan Schieman (ARSC) for helium pycnometry measurements and thermal analysis, Linda McCorkle (Ohio Aerospace Institute) for SEM images, and Anna Palczer for nitrogen sorption measurements. We also thank the Third Frontier Program of the State of Ohio for funding the construction of the roll to roll film manufacturing line.

## REFERENCES

(1) Pierre, A. C.; Pajonk, G. M. *Chem. Rev.* **2002**, *102*, 4243–4265.
(2) For a recent review,see Randall, J. P.; Meador, M. A. B.; Jana, S. C. *ACS Appl. Mater. Interfaces* **2011**, 3, 613–626.
(3) Meador, M. A. B.; Scherzer, C. M.; Nguyen, B. N.; Quade, D.; Vivod, S. L. *ACS Appl. Mater. Interfaces* **2010**, *2*, 2162–2168.

(4) Meador, M.A.B.; Capadona, L.A.; McCorkle, L.; Papadopoulos, D. S.; Leventis, N. *Chem. Mater.* **2007**, *19*, 2247−2260.
(5) Boday, D. J.; Stover, R. J.; Muriithi, B.; Keller, M. W.; Wertz, J. T.; Obrey, K. A. D.; Loy, D. A. *ACS Appl. Mater. Interfaces* **2009**, *1*, 1364−1369.
(6) Nguyen, B. N.; Meador, M. A. B.; Tousley, M. E.; Shonkwiler, B.; McCorkle, L.; Scheiman, D. A.; Palczer, A. *ACS Appl. Mater. Interfaces* **2009**, *1*, 621−630.
(7) Braun, R. D.; Manning, R. M. *J. Spacecr. Rockets* **2007**, *44*, 310−323.
(8) Reza, S.; Hund, R.; Kustas, F.; Willcockson, W.; Songer, J. *9th AIAA Aerodynamic Decelerator Systems Technology Conference and Seminar*; Williamsburg, VA, May 21−24, 2007 ; AIAA: Reston, VA, 2007; 2516.
(9) Brown, G. J.; Lingard, J. S.; Darley, G. D.; Underwood, J. C. *19th AIAA Aerodynamic Decelerator Systems Technology Conference and Seminar*; Williamsburg, VA, May 21−24, 2007 ; AIAA: Reston, VA, 2007; 2543.
(10) Cassidy, P. E. *Thermally Stable Polymers*; Marcel Dekker: New York, 1980.
(11) Meador, M. A. *Annu. Rev. Mater. Sci.* **1998**, *28*, 599−630.
(12) Hergenrother, P. M. *High Perform. Polym.* **2003**, *15* (1), 3−45.
(13) Rhyne, W.; Wang, J.; Begag, R. U.S. Patent WO/2004/009673, Jan. 29, 2004.
(14) Chidambareswarapattar, C.; Larimore, Z.; Sotiriou-Leventis, C.; Mang, J. T.; Leventis, N. *J. Mater. Chem.* **2010**, *20*, 9666−9678.
(15) Kawagishi, K.; Saito, H.; Furukawa, H.; Horie, K. *Macromol. Rapid Commun.* **2007**, *28*, 96−100.
(16) Meador, M. A. B.; Malow, E. J.; He, Z. J.; McCorkle, L.; Guo, H.; Nguyen, B. N. *Polym. Prepr.* **2010**, *51*, 265−266.
(17) Guo, H.; Meador, M. A. B.; McCorkle, L.; Quade, D. J.; Guo, J.; Hamilton, B.; Cakmak, M.; Sprowl, G. *ACS Appl. Mater. Interfaces* **2011**, *3*, 546−552.
(18) Del Corso, J. A..; Cheatwood, F. M.; Bruce, W. E.; Hughes, S. J.; Calomino, A. M., 2011, *21st AIAA Aerodynamic Decelerator Systems Technology Conference and Seminar*; Dublin, Ireland, May 23−26, 2011 ; AIAA: Reston, VA, 2011; 2510.
(19) Takeichit, T.; Stille, J. K. *Macromolecules* **1986**, *19*, 2093−2102.
(20) Meador, M. A. B.; Cubon, V. A.; Scheiman, D. A.; Bennett, W. R. *Chem. Mater.* **2003**, *15*, 3018−3025.
(21) Peter, J.; Kosmala, B.; Bleha, M. *Desalination* **2009**, *245* (1-3), 516−526.
(22) Energy minimizationcalculations using MM2 were made using ChemPro 3D version 12 fromCambridgeSoft using a modification of Allinger's Force Fieldmethod as described in Dudek, M.J.; Ponder, J.W. *J. Comput. Chem.* **1995**, *16*, 791−816.
(23) Chuang, K. C.; Kinder, J. D.; Hull, D. L.; McConville, D. B.; Youngs, W. J. *Macromolecules* **1997**, *30*, 7183−7190.
(24) Coburn, J. C.; Soper, P. D.; Auman, B. C. *Macromolecules* **1995**, *28*, 3253−3260.
(25) Kim, Y. H.; Kim, H. S.; Kwon, S. K. *Macromolecules* **2005**, *38*, 7950−7956.
(26) Ritter, N.; Senkovska, I.; Kaskel, S.; Weber, J. *Macromolecules* **2011**, *44*, 2025−2033.
(27) Brunauer, S.; Emmett, P. H.; Teller, E. *J. Am. Chem. Soc.* **1938**, *60*, 309.
(28) Katti, A.; Shimpi, N.; Roy, S.; Lu, H.; Fabrizio, E. F.; Dass, A.; Capadona, L. A.; Leventis, N. *Chem. Mater.* **2006**, *18*, 285−296.
(29) Gross, J.; Fricke, J. *Nanostruct. Mater.* **1995**, *6*, 905−908.
(30) Ma, H. S.; Roberts, A.; Prevost, J. H.; Jullien, R.; Scherer, G. W. *J. Non-Cryst. Solids* **2000**, *277*, 127−141.
(31) Meador, M. A. B.; Fabrizio, E. F.; Ilhan, F.; Dass, A.; Zhang, G.; Vassilaras, P.; Johnston, J. C.; Leventis, N. *Chem. Mater.* **2005**, *17*, 1085−1098.
(32) For example, see Ehlers, G. F. L, Soloski, E. J. *Thermal Analysis of Polymers in Air*; Technical report AFML-TR-78-64 ; Air Force Materials Laboratory: Wright-Patterson AFB, OH, 1978.
(33) Dine-Hart, R. A.; Wright, W. W. *Makromol. Chem.* **1972**, *153*, 237−254.
(34) Critchley, J. P.; Knight, G. J. ; Wright, W. W. *Heat Resistant Polymers*; Plenum Press: New York, 1983.